CHARACTERIZATIONS AND ANTIBACTERIAL PROPERTIES OF ZnS/ZnO CORE-SHELL STRUCTURES ON SILVER WIRES

H. CHEN[a*], W. M. SU[a], C.Y. WENG[a], W. C. WENG[a], Y. S. TSAI[a], Y. T. CHEN[a], C. C. LU[a], Y. T. A. LIAO[b], C. T. R. YU[b], F. LIN[c], Y. S. LIN[d]

[a]*Department of Applied Material and Optoelectronic Engineering, National Chi Nan University, Taiwan, ROC*

[b]*Department of Applied Chemistry, National Chi Nan University, Taiwan, ROC*

[c]*Department of Materials Science and Engineering, National Chung Hsing University, Taiwan, ROC*

[d]*Department of Chemical Engineering, Feng Chia University, Taiwan, ROC*

In this study, ZnS/ZnO coreshell structures were electro-hydrothermally deposited on silver wires. To analyze the properties of the ZnS/ZnO nanostructures on silver wires, multiple material, optical, and biomedical analyses including FESEM, EDX, FTIR, XPS, and antibacterial effects were conducted. Multiple characterization results indicate that ZnS/ZnO shell could be optimally grown on silver at an appropriate deposition time. In line with the material characterizations, the best antibacterial effects exhibited at the ZnS growth time of 10 minutes. ZnO/ZnS/silver structures are promising for future biomedical antibacterial applications

(Received August 4, 2017; Accepted November 10, 2017)

Keywords: Silver wire, Core-shell structure, ZnS/ZnS, Antibacterial, Nanostructure

1. Introduction

ZnO sulfide/zinc oxide (ZnS/ZnO) nanostructures have been intensity studied due to their distinct material and optical properties [1-3]. Zinc sulfide is a non-toxic semiconductor with a direct wide band gap [4, 5], so that incorporating ZnS on ZnS nanorods (NRs) to form the ZnS/ZnO coreshell structures can have versatile optical and catalytic application [6-8]. Since ZnO NRs fabricated on the silver wire have been reported as light sensor [9], opto-isolator [10], and biosensor applications [11,12]. Including the core shell of ZnS [13,14] may further enhance the biomedical performance of the nanostructures on silver wires [15-18]. Based on literature research, one study has grown ZnS also directly on the silver structure [19]. However, ZnS/ZnO/silver structures have not been clearly reported yet. In this study, ZnO NRs were firstly grown on silver wires [20] and then the ZnO NRs/silver wire structures were coated with ZnS shell to form the ZnS/ZnO coreshell structures. To characterize the core-shell structures, multiple characterizations [21] were performed. Field-emission scanning electron microscope (FESEM) was used to view the morphology of the core-shell structures, energy dispersive spectrometer (EDS) was used to examine the element compositions, and X-ray diffraction (XRD) was used to observe the crystalline structures. X-ray photoelectron spectroscopy (XPS) and Fourier-transform infrared spectrometer (FTIR) were conducted to examine the chemical bindings. Finally, OD 600 antibacterial tests can be applied to evaluate the antibacterial effects. Results indicate that ZnS with deposition time of 10 minutes had the strongest crystalline structures and sulfur contents. Corresponding with the material analyses, ZnS/ZnO/silver wires with ZnS deposition time of 10 minutes exhibited the strongest antibacterial properties. ZnO/ZnS core-shell structures on silver

*Corresponding author: hchen@ncnu.edu.tw

wires with appropriate ZnS growth time show promise for future biomedical antibacterial applications.

2. Experimental procedure

To fabricate ZnS/ZnO core-shell structures on silver wires, we prepared five silver wires with a diameter of 2mm and a length of 3 cm in size as shown in Fig. 1(a) and (b). The wires were cleansed with ethanol, acetone, and isopropyl alcohol for 10 minitues. After that, we put five silver wires into a 100 ml solution containing 0.1 M zinc nitrate and 0.1M potassium nitrate, and then electro-deposited zinc oxide seed layers on the silver wires with a current of 18mA for 12 seconds one by one . After that, the five wires containing the seed layer was placed in serum bottle with a 100 mal solution containing 0.05 M zinc nitrate hexahydrate and 0.07 M hexamethylenetetramine to hydrothermally grow ZnO NRs on silver wires at 85° C for one hour.

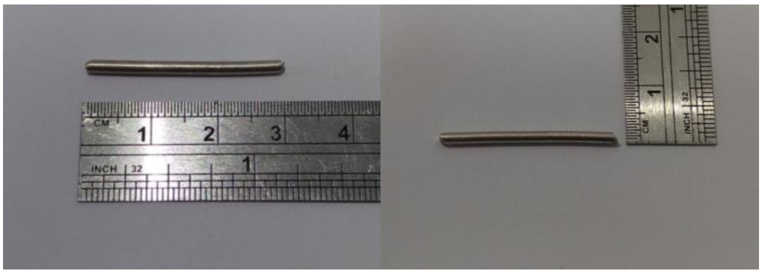

a) *b)*

Fig. 1. Photos of a silver wire with (a) 3 cm length and (b) 2 mm diameter.

Then, four samples were put in the solution containing 0.1 M sodium sulfide nonahydrate100 ml and immersed for 5, 10, 15, and 20 minutes at 65° C, respectively. ZnS/ZnO core-shell structures can be obtained by S^{2-} exchange O^{2-} during hydrothermal growth as shown in equation below.

$$ZnO+2(OH)^{-} \rightleftharpoons ZnO_2^{2-}+H_2O$$

$$ZnO_2^{2-}+S^{2-}+2H_2O \rightleftharpoons ZnS+4(OH)^{-}$$

3. Results and discussion

To observe the ZnS/ZnO core-shell structures, FESEM images of various magnification rates and EDS analyse of the ZnS/ZnO/silver wires with ZnS deposition time of 0, 5, 10, 15, and 20 minutes are shown in Fig. 2 (a), (b), (c), (d), and (e), respectively. FESEM results indicate that fluffy ZnS structures could be successfully grown on the ZnO NRS/sivler wires. In addition, ZnS core-shell could be clearly seen as the ZnS growth time was increased to 10 and 15 minutes. Furthermore, sulfur content could be clearly observed as a ZnS layer was coated on ZnO NRs indicative of reaction and interchanging between S^{2-} and ZnO_2^{2-} to form ZnS/ZnO core-shell structures

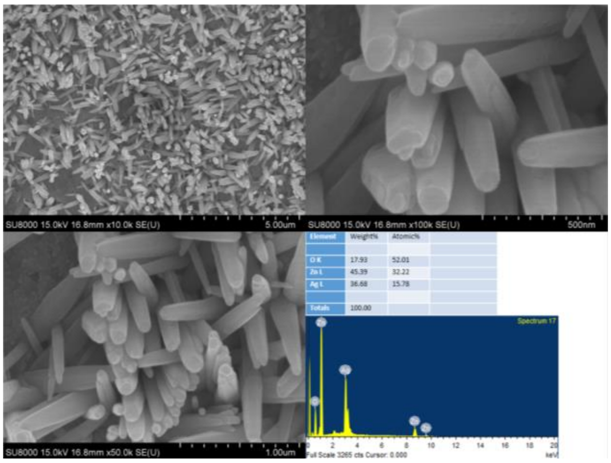

Fig. 2a. FESEM images of various magnification rates and EDS analysis of the ZnS/ZnO core-shell nanostructures with deposition time of (a) 0 min

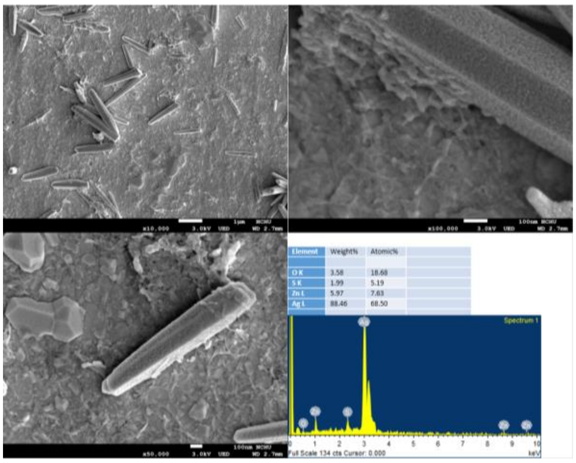

Fig. 2b. FESEM images of various magnification rates and EDS analysis of the ZnS/ZnO core-shell nanostructures with deposition time of (b) 5 mins

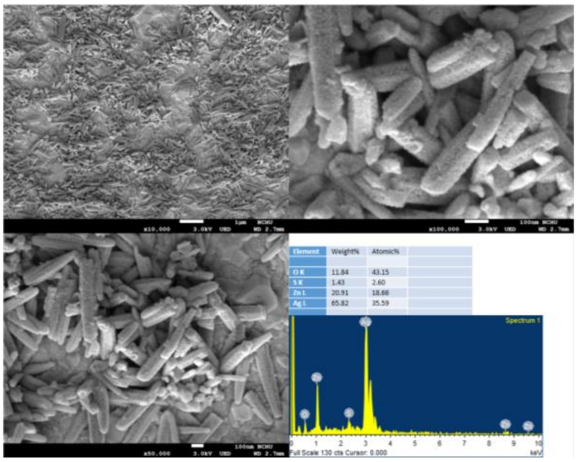

Fig. 2c. FESEM images of various magnification rates and EDS analysis of the ZnS/ZnO core-shell nanostructures with deposition time of (c) 10 mins

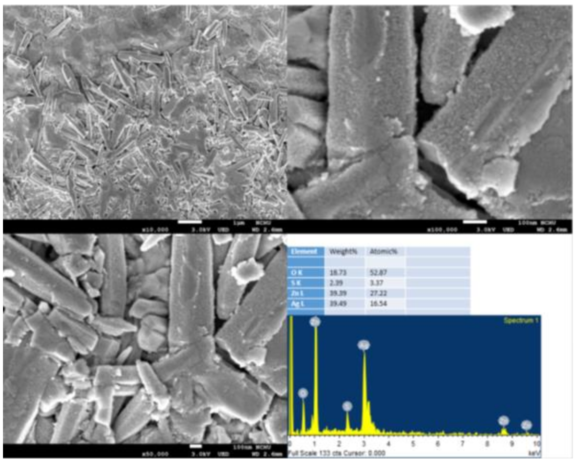

Fig. 2d. FESEM images of various magnification rates and EDS analysis of the ZnS/ZnO core-shell nanostructures with deposition time of (d) 15 mins

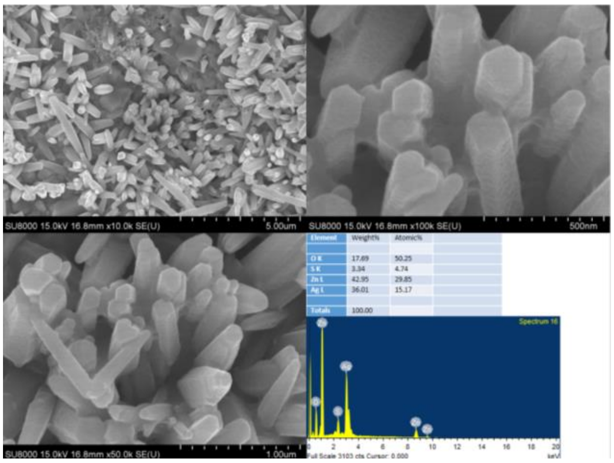

Fig. 2e. FESEM images of various magnification rates and EDS analysis of the ZnS/ZnO core-shell nanostructures with deposition time of (e) 20 mins.

Moreover, to confirm the appearance of the ZnS crystalline structures, XRD was used to examine as shown in Fig. 3(a) and (b). Since the ZnS structures may not be as strong as ZnO and silver, ZnS could not be observed in 20 to 80 degree XRD patterns but the crystal structure of the zinc oxide NRs on the silver wire could be observed by in Fig. 3(a). Therefore, we focused the XRD patterns between 20 to 30 degree as shown in Fig. 3(b). Results show that ZnS (111) crystalline structures could be observed. Moreover, the strong crystalline structures could be seen at the deposition time of 10 and 15 minutes and the strongest ZnS (111) peak could be observed for the ZnS deposition time of 10 minutes.

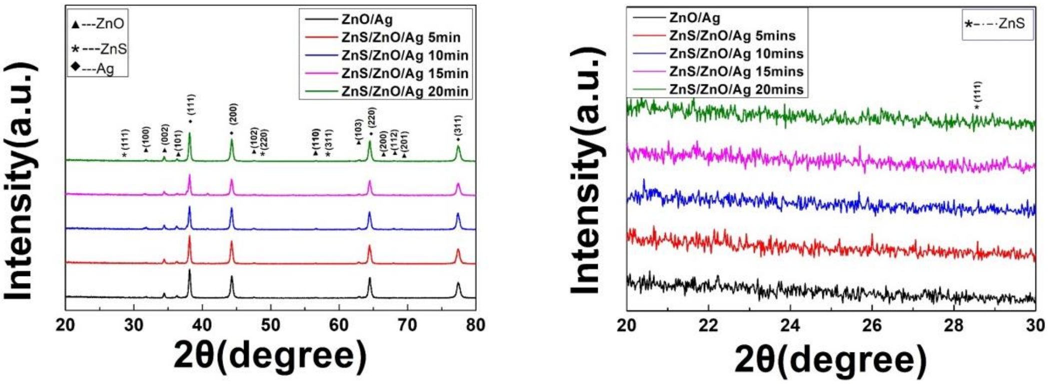

a) *b)*

Fig. 3.(a) 20-80° XRD patterns of the ZnS/ZnO/silver wires with various ZnS deposition time (b) 20-30° XRD patterns of the ZnS/ZnO/silver wires with various ZnS deposition time

Moreover, to evaluate the chemical bindings of the ZnS core-shell structures, XPS was used to study the ZnS bindings as shown in Fig. 4. In line with previous characterizations, sulfur bindings of ZnS/ZnO structures with ZnS deposition could be observed. Moreover, the strongest ZnS binding could be seen for the ZnS deposition time for 10 minutes as shown in Fig. 4, showing that the appropriate time of ZnS growth was 10 minutes.

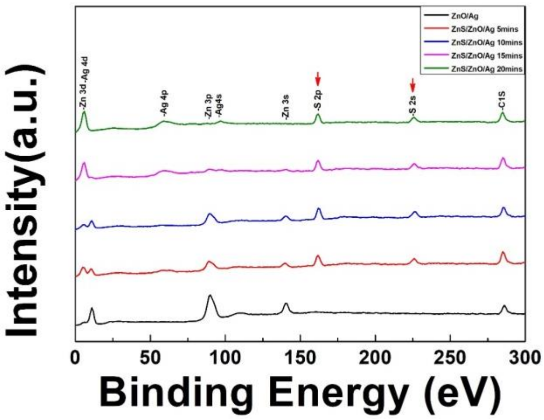

Fig. 4. XPS measurements of ZnS/ZnO/silver wires with various ZnS deposition time.

To further investigate the functional groups contained in the samples, FTIR was used for analysis for the ZnS/ZnO and ZnO strucutres as shown in Fig. 5(a) and (b), respectively. As for Fig. 5(a), the pink point was with ZnS/ZnO deposition and the blue point was with the uncoated silver wire. Apparently, ZnS could be clearly detected with the signal around 1450 cm^{-1} and no ZnS signal appeared for the bare silver wire. Moreover, for Fig 5.(b) with only ZnO NR deposition, no ZnS peak could be seen as well [22, 23]. In addition, peak intensity around 2350 cm^{-1} was C-O signaland peak intensity near 3500-3900 cm^{-1}.

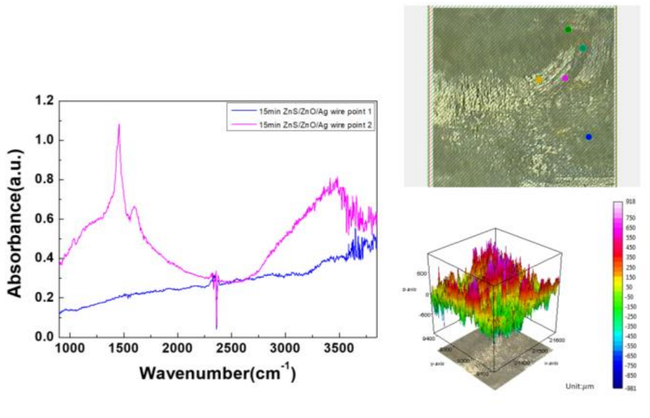

a)

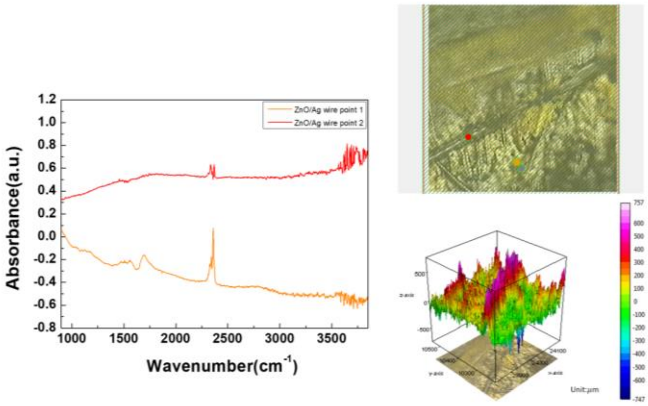

b)

Fig. 5. FTIR measurement of (a) a ZnS/ZnO/silver wire and (b) a ZnO/silver wire.

Finally, OD 600 antibacterial tests were studied for antibacterial effects of the a ZnO/silver wire and ZnS/ZnO/silver wires with ZnS deposition time for 5, 10, 15, and 20 minutes. To study antimicrobial activity, the above five samples were immersed in a solution prepared from E. coli bacteria in the growth medium, while the solution was prepared from the E. coli bacterial growth media. Furthermore, the bacterial density of the collected bacterial solution was detected with spectrophotometer with 600 nm light optical density. Corresponding with all the previous measurements, the ZnS/ZnO/silver wire with ZnS deposition time of 10 minutes had the strongest antibacterial effect indicating that ZnS had the antibacterial properties. This result was consistent with all the previous analyses because ZnS contributed to strengthening of the antibacterial effect [24], and reached the extreme value in 10 minutes. After the growth time of 10 minutes, ZnS gradually disintegrated so that the antibacterial effect was reduced.

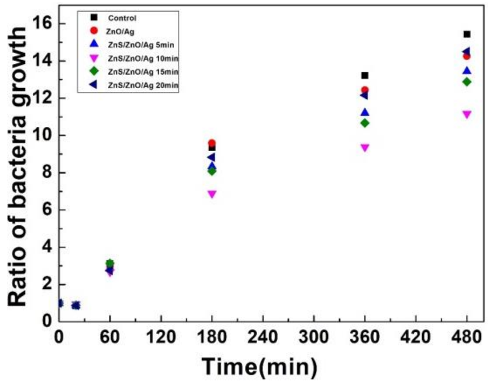

Fig. 6. OD 600 antibacterial tests for the ZnS/ZnO/silver wires with various ZnS deposition time

4. Conclusions

In this paper, ZnS/ZnO core-shell structure on the silver wires were fabricated. To evaluate the properties of ZnS/ZnO/silver wires, multiple analyzes were carried out. Results indicate that ZnS could be properly grown on ZnO NRs/silver wires with the ZnS deposition time of 10 minutes. Furthermore, the antibacterial OD 600 tests reveal that ZnS had antibacterial properties and the core-shell structure with deposition time of 10 minutes had the strongest antibacterial properties. ZnO/ZnS/silver wires with appropriate ZnS deposition time are promising for future biomedical antibacterial applications

Acknowledgements

This work has been supported in part by the Ministry of Science and Technology of Taiwan, ROC under Contract No: MOST 104-2221-E-260-002 -MY3.

References

[1] S.-C. Huang, K. M. Hsieh, T. W. Chang, Y. C. Chen, C.-T. R. Yu, T.-C. Lu, C. F.Lin, T.-Y. Yu, T.-T. Wang, H. Chen, Ceramics international **42**(6), 7848 (2016).
[2] N. Saito, H. Haneda, T. Sekiguchi, N. Ohashi, I. Sakaguchi, K. Koumoto, Advanced Materials **14**(6), 418 (2002).
[3] I. Kazeminezhad, A. Sadollahkhani, Materials Letters **120**, 267 (2014).
[4] R. John, S. Florence, Chalcogenide letters **7**(4), 283 (2010).
[5] M. Sookhakian, Y. Amin, W. Basirun, M. Tajabadi, N. Kamarulzaman, Journal of Luminescence **145**, 244 (2014).
[6] M.-K. Tsai, W. Huang, S.-Y. Hu, J.-W. Lee, Y.-C. Lee, M.-H. Lee, J.-L. Shen, Micro & Nano Letters **11**(4), 192 (2016).
[7] H. X. Sang, X. T. Wang, C. C. Fan, F. Wang, international journal of hydrogen energy **37**(2), 1348 (2012).
[8] A. Brayek, M. Ghoul, A. Souissi, I. B. Assaker, H. Lecoq, S. Nowak, S. Chaguetmi, S. Ammar, M. Oueslati, R. Chtourou, Materials Letters **129**, 142 (2014).
[9] X. Fang, Y. Bando, U. K. Gautam, T. Zhai, H. Zeng, X. Xu, M. Liao, D. Golberg, Critical Reviews in Solid State and Materials Sciences **34** (3-4), 190 (2009).
[10] L. Hu, J. Yan, M. Liao, H. Xiang, X. Gong, L. Zhang, X. Fang, Advanced Materials **24**(17), 2305 (2012).

[11] A. K. Giri, C. Charan, A. Saha, V. K. Shahi and A. B. Panda, Journal of Materials Chemistry A **2**(40), 16997 (2014).
[12] A. Baranowska-Korczyc, K. Sobczak, P. Dłużewski, A. Reszka, B. J. Kowalski, Ł. Kłopotowski, D. Elbaum and K. Fronc, Physical Chemistry Chemical Physics **17**(37), 24029 (2015).
[13] T. Serrano, J. Cavazos, Y. Peña and I. Gómez, Chalcogenide Letters **11**(1), 21 (2014).
[14] N. Soltani, E. Saion, M. Erfani, A. Bahrami, M. Navaseri, K. Rezaee, M. Z. Hussein, Chalcogenide Letters **9**(9) 379, (2012).
[15] S. Tarish, A. Al-Haddad, R. Xu, D. Cao, Z. Wang, S. Qu, G. Nabi and Y. Lei, Journal of Materials Chemistry C **4**(7), 1369 (2016).
[16] X. Huang, M. Wang, M.-G. Willinger, L. Shao, D. S. Su, X.-M. Meng, ACS nano **6**(8), 7333 (2012).
[17] J. Rouhi, C. R. Ooi, S. Mahmud, M. R. Mahmood, Materials Letters **147**, 34 (2015).
[18] T. Yu, K. Wang, Y. Chen, M. Sheu, H. Chen, Chalcogenide Letters **14**(4), 119 (2017).
[19] W. Jian, J. Zhuang, D. Zhang, J. Dai, W. Yang, Y. Bai, Materials chemistry and physics **99** (2), 494 (2006).
[20] H. Chen, W. M. Su, Y.-T. Chen, C.-C. Lu, C.-Y. Weng, Journal of New Materials for Electrochemical Systems **20**(2), 049 (2017).
[21] C.-H. Kao, H. Chen, L.-T. Kuo, J.-C. Wang, Y.-T. Chen, Y.-C. Chu, C.-Y. Chen, C.-S. Lai, S. W. Chang, C. W. Chang, Sensors and Actuators B: Chemical **194**, 419 (2014).
[22] G. Janita Christobel, International Journal of Science and Research **5** (4), 2319 (2016).
[23] I. Parvaneh, S. Samira and N. Mohsen, Chinese Physics B **24** (4), 046104 (2015).
[24] N. Parvin, G. Amiri, V. Karbasizadeh, Nanomedicine Journal **3** (3), 191 (2016).